PHYSICAL REVIEW B **84**, 121303(R) (2011)

Absence of intrinsic spin splitting in one-dimensional quantum wires of tetrahedral semiconductors

Jun-Wei Luo,[1,*] Lijun Zhang,[1] and Alex Zunger[2,†]
[1]*National Renewable Energy Laboratory, Golden, Colorado 80401, USA*
[2]*University of Colorado, Boulder, Colorado 80309, USA*
(Received 15 June 2011; published 12 September 2011)

The energy bands of three-, two-, and one-dimensional (1D) structures are generally split at certain wave-vector values into spin components, a spin splitting (SS) that occurs even without an external magnetic field and reflects the effect of spin-orbit interaction on certain symmetries. We show via atomistic theory that 1D quantum wires made of conventional zinc-blende semiconductors have unexpected zero SS for all electron and hole bands if the wire is oriented along (001) (belonging to D_{2d} symmetry), and for some of bands if the wire is oriented along (111) (belonging to C_{3v} symmetry). We find that the predicted absence of a Dresselhaus SS in both (001)-oriented and (111)-oriented 1D wires is immune to perturbations lowering their original D_{2d} and C_{3v} structural symmetries, such as alloying of the matrix around the wire or application of an external electric field. Indeed, such perturbations induce only a Rashba SS. We find that the scaling of the SS with the wave vector is dominated by a linear term plus a minor cubic term.

DOI: 10.1103/PhysRevB.84.121303 PACS number(s): 73.21.Fg, 71.70.Ej, 71.15.−m

In the presence of the spin-orbit interaction (SOI), an electron moving in the inversion-symmetry-breaking electric field feels an internal effective magnetic field $\mathbf{B}_{\text{in}}(\mathbf{k})$ which leads to splitting of the spin degeneracy of energy bands along certain wave-vector directions $\mathbf{k}$. The inversion-symmetry-breaking electric field can arise either from the *intrinsic* bulk inversion asymmetry (a Dresselhaus SOI)[1] or from an *extrinsic* structural inversion asymmetry (a Rashba SOI).[2] Such a SOI hence provides certain control on the electron spin through the manipulation of electron motion and plays a central role in spintronics[3–9] as well as topological insulators.[10,11]

The absence or presence of intrinsic spin splitting (SS) at a given k point in a particular structure and dimensionality can be obtained from symmetry, as we illustrate in Fig. 1, where we give all irreducible representations $\gamma_i^{(\lambda)}$ (with degeneracy λ) of the point group of k points along high-symmetry k lines for three-dimensional (3D) bulk zinc-blende structures, two-dimensional (2D) quantum wells (QWs), and one- dimensional (1D) quantum wires. In double group representations including spin,[1] a band belonging to a representation with dimension $\lambda \geqslant 2$ has no SS (spin degeneracy) and spin degeneracy is lifted in a band if it belongs to a representation with dimension $\lambda = 1$. Therefore, two general cases are noteworthy in Fig. 1, relating to the absence (presence) of SS to the degeneracy $\lambda = 2$ ($\lambda = 1$): (i) If the point group of a k point contains only representations with dimension $\lambda = 2$, then there is no spin splitting for any bands at this k point. Thus, a 3D zinc-blende bulk structure has no SS along [100]. (ii) If the point group of a k point contains only single-degenerate ($\lambda = 1$) representations, there is SS for every band at this k point, e.g., k points along [110] (Γ-K) in zinc-blende structures.[1]

We see that the absence or presence of intrinsic SS is a general physical feature anchored in the symmetry properties of the underlying states, as first discussed by Dresselhaus.[1] However, the prediction of the magnitude of SS, when it is nonzero, as well as the determination of its scaling with the wave vector k (linear versus cubic) requires an atomistic approach, capable of resolving the correct symmetry of the object at hand. The scaling is understood for 3D and 2D but not for 1D: In 3D bulk zinc-blende structures the cubic term is the lowest order of electron Dresselhaus SS.[1] In 2D QWs, besides cubic terms, a linear term appears due to a quantized wave vector in the growth direction.[12] In contrast to 3D bulk and 2D QWs, far less attention has been devoted to understanding the SOI-induced SS in 1D quantum wires. Indeed, it has not been determined if SS exists at all in certain 1D structures, and what is the scaling with momentum. Ignoring the atomistic symmetry, $\mathbf{k}\cdot\mathbf{p}$ calculations[13–17] have postulated sometimes only linear and sometimes both linear and cubic Dresselhaus terms in their model Hamiltonian.

In this Rapid Communication we (i) use symmetry (Fig. 1) to establish the rigorous absence of intrinsic SS in (001)-oriented 1D zinc-blende quantum wires, where the SS vanishes identically for all electron and hole bands. In addition, in (111)-oriented 1D quantum wires, SS vanishes for part of bands including the lowest conduction band (CB1) and highest valence band (VB1). (ii) We find that this symmetry-enforced vanishing of Dresselhaus SS is immune to symmetry lowing factors such as random alloy fluctuations of the wire matrix or application of an external electric field perpendicular to the wire; these factors introduce only Rasbha SOI-induced SS. (iii) Applying atomistic electronic structure calculations we find the magnitude and scaling of the intrinsic SS with the wave vector. The scaling is dominated by a linear term plus a minor cubic term.

Approach. We calculate SS in the (001)-, (110)-, and (111)-oriented 1D GaAs/AlAs quantum wires which have a cross section with GaAs atoms inside the atom-centered circle with radius R and AlAs atoms outside. We use a lattice constant $a = 5.653$ Å for both GaAs and AlAs, neglecting the slight lattice mismatch. Since the origin of intrinsic SS lies in the atomic-scale (a)symmetry, we avoid a geometric continuum description underlying the few-band $\mathbf{k}\cdot\mathbf{p}$. Unable to resolve atomic symmetry,[18] such approaches add intrinsic SS essentially "by hand" (sometimes guessing it incorrectly[19]). Instead, we describe the (screened) electron-ion potential $V(\mathbf{r})$ of the system (3D, 2D, or 1D) as a superposition of atom-centered potentials v_α of all atoms in the system, thus

Dim.	Str.	PG	k=[001]	k=[100]	k=[110]	k=[1$\bar{1}$0]	k=[111]
3D	ZB Bulk	T_d	C_{2v} $\gamma_5^{(2)}$	C_{2v} $\gamma_5^{(2)}$	C_s $\gamma_3^{(1)} \oplus \gamma_4^{(1)}$	C_s $\gamma_3^{(1)} \oplus \gamma_4^{(1)}$	C_{3v} $\gamma_4^{(2)} \oplus \gamma_5^{(1)} \oplus \gamma_6^{(1)}$
2D	(001) QWell	D_{2d}	nd	C_s $\gamma_3^{(1)} \oplus \gamma_4^{(1)}$	C_2 $\gamma_3^{(1)} \oplus \gamma_4^{(1)}$	C_2 $\gamma_3^{(1)} \oplus \gamma_4^{(1)}$	nd
	(110) QWell	C_{2v}	C_{2v} $\gamma_5^{(2)}$	nd	nd	C_s $\gamma_3^{(1)} \oplus \gamma_4^{(1)}$	nd
	(111) QWell	C_{3v}	nd	nd	nd	C_1 $\gamma_2^{(1)}$	nd
1D	(001) QWire	D_{2d}	C_{2v} $\gamma_5^{(2)}$	nd	nd	nd	nd
	(110) QWire	C_{2v}	nd	nd	C_s $\gamma_3^{(1)} \oplus \gamma_4^{(1)}$	nd	nd
	(111) QWire	C_{3v}	nd	nd	nd	nd	C_{3v} $\gamma_4^{(2)} \oplus \gamma_5^{(1)} \oplus \gamma_6^{(1)}$

FIG. 1. (Color online) The subgroup and representations of k points along the wave-vector directions [001], [100], [110], [1$\bar{1}$0], and [111] for 3D zinc-blende (ZB) structures, 2D quantum wells, and 1D quantum wires accompanying the point group (PG) of the structures. There are three real-space orientations (001), (110), and (111) for 2D quantum wells and 1D quantum wires. The degeneracy of each representation is presented as its superscript in parentheses. We adopt the Koster-Dimmock-Wheeler-Statz notation (Ref. 26) for representations of the symmetry double group.

forcing upon us the correct atomically resolved symmetry. The single-particle Schrödinger equation associated with $V(\mathbf{r})$ is then solved in a general plane-wave basis set whose size is selected so that it does not affect the answer. Hence, the results are equally applicable to any wave vector (not just small k), and all-band as well as all-valley coupling are naturally included. In practice, $V(\mathbf{r})$ is taken as a superposition of overlapping potentials $\hat{v}_\alpha(\mathbf{r})$ of the constituent atoms,[20,21]

$$V(\mathbf{r}) = \sum_n \sum_\alpha \hat{v}_\alpha(\mathbf{r} - \mathbf{R}_n - \mathbf{d}_\alpha), \tag{1}$$

where $\hat{v}_\alpha(\mathbf{r} - \mathbf{R}_n - \mathbf{d}_\alpha)$ pertains to atom type α at site $\mathbf{d}_\alpha$ in the nth primary cell $\mathbf{R}_n$. The symmetry of the structure is hence expressed in an explicit manner via atomic positions. The construction of $\hat{v}_\alpha$ is the key to accuracy and realism. To remove the "local density approximation (LDA) error" in the bulk crystal, we fit $\hat{v}_\alpha$ to reproduce well not only the bulk band gaps throughout the zone, but also the electron and hole effective-mass tensors, as well as the valence- and conduction-band offsets between two materials in a heterostructure, the spin-orbit splitting, and the hydrostatic and biaxial deformation potentials.[19,21,22] The construction of $V(\mathbf{r})$ and its accuracy has been described in Refs. 21 and 22. This approach has been previously applied to SS in 3D bulk GaAs (Ref. 22) and in 2D (001) GaAs/AlAs quantum wells.[19] The linear and cubic terms of numerically calculated SS $\Delta_i(\mathbf{k})$ of band i is obtained by fitting it to a power series in k,

$$\Delta_i(\mathbf{k}) = \alpha_i k + \gamma_i k^3. \tag{2}$$

Intrinsic spin splitting in 1D wires. The band structure of (001)-, (110)-, and (111)-oriented 1D GaAs/AlAs quantum wires near the Brillouin zone center $\bar{\Gamma}$ is shown in Fig. 2. The

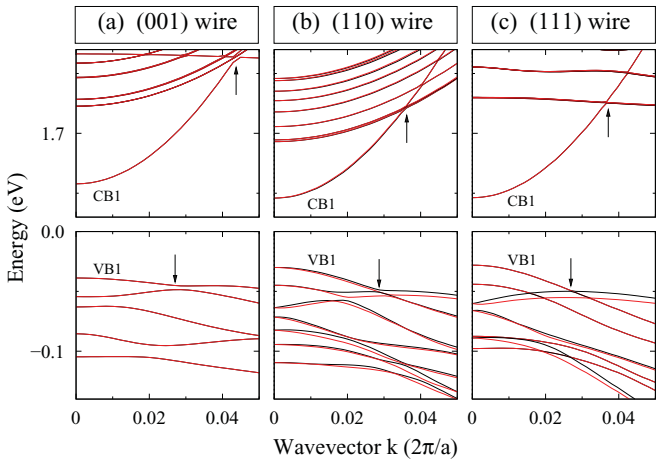

FIG. 2. (Color online) Band structure of (a) (001)-, (b) (110)-, and (c) (111)-oriented GaAs/AlAs quantum wires with radius $R = 4.0$ nm. Red (gray) and black denote different spin bands for each orbital band, which are hardly resolved visually on this energy scale. Vertical arrows indicate the band crossing (or anticrossing) of the lowest conduction band (CB1) and the highest valence band (VB1).

two spin components of each orbital band are represented by red (gray) and black lines, respectively. For the (001) wire in Fig. 2(a) one observes a single color for all bands because $\Delta_i(\mathbf{k}) = 0$. For the (110) wire in Fig. 2(b) both red (gray) and black lines are seen for every band, since there is SS for all bands. However, in (111)-oriented wire, as shown in Fig. 2(c), some bands, including CB1 and VB1, have no SS and others have SS. Figure 3 shows SS (defined as the absolute energy difference between two spin components for each orbital band) of both CB1 (top panels) and VB1 (bottom panels) for three wire orientations. Indeed, Fig. 3(a) shows zero SS for both CB1 and VB1 in (001)-oriented 1D wire and Fig. 3(b) shows large SS for both CB1 and VB1 in (110)-oriented 1D wire.

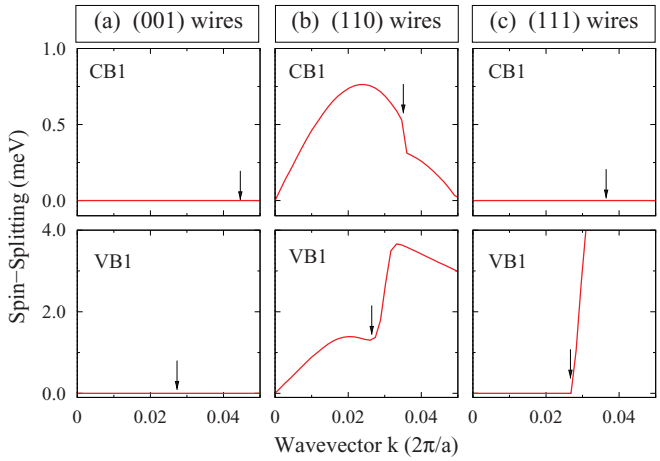

FIG. 3. (Color online) Spin splitting of (a) (001)-, (b) (110)-, and (c) (111)-oriented GaAs/AlAs quantum wires with radius $R = 4.0$ nm. The top panels are for the lowest conduction band (CB1) and the bottom panels are for the highest valence band (VB1). The vertical arrows indicate the band crossing of CB1 or VB1.

However, Fig. 3(c) shows different results for (111)-oriented 1D wire: In the valence bands the (111) wire shows no SS for VB1 in the small-k region, but SS appears suddenly at a critical k point [$\sim 0.03(2\pi/a)$]. The transition between the absence and presence of SS in VB1 is due to band crossing (marked by arrows in Fig. 2). As shown in Fig. 2(c), VB1 and VB2 in the (111) wire have no SS but VB3 does exhibit SS. At $k \sim 0.03(2\pi/a)$ there is a band crossing between VB1 and VB3, hence there is a transition from the absence of SS to the presence of SS. In the conduction bands of the (111) wire, band crossing between the CB1 and CB2 bands does not contribute to a similar transition of SS since both CB1 and CB2 bands have no SS [the observed SS in Fig. 2(c) is arising from CB3, which is almost degenerate with CB2].

Atomistic symmetry and spin splitting. It is interesting to note the absence of SS in 1D wires as opposed to the presence of SS in the corresponding 2D QWs and 3D bulk structures. To understand this phenomena we analyze in Fig. 1 the symmetry of k points along high-symmetry k lines in 1D, 2D, and 3D structures with real-space lattice orientations (001), (110), and (111). Figure 1 indicates the point-group (PG) symmetry of each structure, which is T_d for 3D bulk, and D_{2d} for the (001) wire and well, C_{2v} for the (110) wire and well, and C_{3v} for the (111) wire and well. Next, Fig. 1 indicates the **k** directions where there are no band dispersion ("nd"), hence no SS. In the remaining **k** directions that manifest band dispersion, we give the symmetry representations $\gamma_i^{(\lambda)}$. We find the following from Fig. 1: (a) In 3D bulk zinc-blende structures with T_d symmetry, SS exists for all bands along the $\mathbf{k} = [110]$ and $\mathbf{k} = [1\bar{1}0]$ directions since there $\lambda = 1$ and for some of bands along $\mathbf{k} = [111]$ since there $\lambda = 1, 2$. (b) In (001)-oriented 2D QWs, SS exists for all bands in all the in-plane directions since there $\lambda = 1$. (c) In (110)-oriented 2D QWs, there exist finite SS Δ_i for all bands along the in-plane $\mathbf{k} = [1\bar{1}0]$ direction since there $\lambda = 1$, but Δ_i vanishes along the in-plane $\mathbf{k} = [001]$ direction since there $\lambda = 2$. (d) In (111)-oriented 2D QWs, there exist finite SS in all in-plane directions since there $\lambda = 1$. (e) In 1D quantum wires there is only a single direction where energy dispersion exists, which is different from the infinite number of dispersing directions as in 2D quantum wells and 3D bulk structures. In (001)-oriented 1D quantum wires, there is no SS for any dispersing bands since $\lambda = 2$. In (110)-oriented 1D quantum wires, there exist finite SS for any dispersing bands since $\lambda = 1$. However, in (111)-oriented 1D quantum wires, both types of λ values exist and hence the bands belonging to $\lambda = 2$ have no SS and other bands belonging to $\lambda = 1$ have SS. The numerical results shown in Figs. 2 and 3 follow this symmetry analysis.

Effects of reduced symmetry. The absence of SS in (001)- and (111)-oriented 1D quantum wires is a result of atomic symmetry. One therefore wonders what would happen if one reduces the atomic symmetry by alloying, or adding surface ligands, or applying an external electric field. This can be examined by randomly alloying the wire matrix to $Al_{0.9}Ga_{0.1}As$ and keeping the wire core as pure GaAs. For (001) wire, this results in the appearance of SS but with a rather small magnitude. Its linear term coefficient α_i (i = CB1, VB1) and cubic term coefficient γ_i (i = VB1) of Eq. (2) (Ref. 23) as a function of wire radius is shown in Figs. 4(a) and 4(b), respectively, as well as that of intrinsic (Dresselhaus) SS of

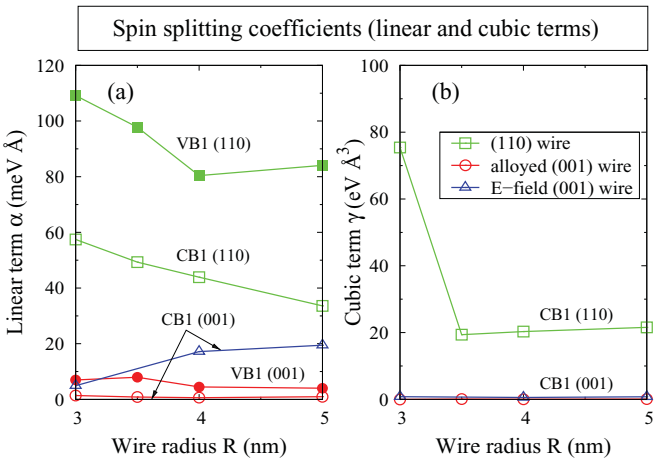

FIG. 4. (Color online) Magnitude of (a) linear term coefficient α_i (i = CB1, VB1) and (b) cubic term coefficient γ_i (i = CB1) of spin splitting terms as a function of wire radius R for (110)-oriented GaAs/AlAs quantum wires (belonging to C_{2v} symmetry) and (001)-oriented $GaAs/Al_{0.9}Ga_{0.1}As$ quantum wires (belonging to C_1 symmetry) as well as (001)-oriented GaAs/AlAs quantum wires (belonging to D_{2d}) by applying an external electric field as large as $E = 10^7$ V/m.

(110) GaAs/AlAs wires. We find that the linear term of both CB1 and VB1 of alloyed (001) wire [Fig. 4(a)], which is dominant in the small-k range, is two orders of magnitude smaller than that of corresponding bands in 1D (110)-oriented wire. This symmetry-lowering-induced SS through alloying of the wire matrix is a Rashba SOI effect rather than a Dresselhaus SOI effect, as evidenced by the fact that its cubic term is extremely small compared with the Dresselhaus SOI cubic term of (110)-oriented wire, as shown in Fig. 4(b). For electron bands, a Rashba SS has only a linear term[2,5] and a Dresselhaus SS has a large cubic term (the magnitude of the cubic term is expected to be the same for 1D, 2D, and 3D according to the single-band model[12,15,24]).

Another way to reduce the D_{2d} symmetry of (001) wire is by applying an external electric field perpendicular to the wire. We apply an electric field as large as 10^7 V/m to the 1D (001) GaAs/AlAs wire. The calculated coefficients of linear and cubic terms α_i and γ_i [i = CB1 (Ref. 25)] are also shown in Figs. 4(a) and 4(b), respectively. Similar to the alloying-induced SS, the E-field-induced SS is linear in k (the cubic term is negligible). This indicates that the external electric field induces only a Rashba SS and does not switch on the intrinsic Dresselhaus SS. By comparing [Fig. 4(a)] the E-field-induced (Rashba) SS of CB1 of (001) wire to the intrinsic (Dresselhaus) SS of CB1 of (110) wire, we see that the Rashba SOI is smaller than the Dresselhaus SOI. This is in contrast to 2D QWs where the Dresselhaus SOI is negligible in comparison with the Rashba SOI.[7,9] We conclude that the predicted absence of a Dresselhaus SS in both (001)- and (111)-oriented 1D quantum wires is immune to the perturbations lowering their original D_{2d} and C_{3v} structure symmetries, such as alloying the wire matrix and applying an external electric field. These induce only the Rashba SS. This conclusion can be applied to intrinsic E fields due to a quantum wire operating as a device, e.g., surface-polarization-induced

field in response to space charge and E field in response to the charge current flowing in the wire.

The absence of a Dresselhaus SS in 1D wires is rather general because it is based on an atomistic symmetry consideration, and thus applies to all zinc-blende wires of the same orientations. This finding is unexpected by the existing literature.[13–17] This result suggests that 1D quantum wires might be promising candidates for spintronic devices because they avoid some of the problems underlying the 2D structures that manifest intrinsic untunable Dresselhaus electron SS.[7,8,11]

This work was funded by the US Department of Energy, Office of Science, Basic Energy Science, Materials Sciences and Engineering, under Contract No. DE-AC36-08GO28308 to NREL.

*jun-wei.luo@nrel.gov
†alex.zunger@gmail.com

[1] G. Dresselhaus, Phys. Rev. **100**, 580 (1955).
[2] Y. A. Bychkov and E. I. Rashba, J. Phys. C **17**, 6039 (1984).
[3] A. Fert, Rev. Mod. Phys. **80**, 1517 (2008).
[4] M. I. Dyakonov and V. I. Perel, Zh. Eksp. Teor. Fiz. **60**, 1954 (1971) [Sov. Phys. JETP **33**, 1053 (1971)].
[5] S. Datta and B. Das, Appl. Phys. Lett. **56**, 665 (1990).
[6] J. Schliemann, J. C. Egues, and D. Loss, Phys. Rev. Lett. **90**, 146801 (2003).
[7] L. Mieier, G. Salis, I. Shorubalko, E. Gini, S. Schön, and K. Ensslin, Nat. Phys. **3**, 650 (2007).
[8] I. Vurgaftman and J. R. Meyer, J. Appl. Phys. **97**, 053707 (2005).
[9] X. Cartoixà, D. Z.-Y. Ting, and Y. C. Chang, J. Supercond. **18**, 163 (2005).
[10] For a review, see X. L. Qi and S. C. Zhang, Physi. Today **63**(1), 33 (2010).
[11] B. A. Bernevig, T. L. Hughes, and S. C. Zhang, Science **314**, 1757 (2006).
[12] R. Eppenga and M. F. H. Schuurmans, Phys. Rev. B **37**, 10923(R) (1988).
[13] S. Pramanik, S. Bandyopadhyay, and M. Cahay, Phys. Rev. B **76**, 155325 (2007).
[14] S. Zhang, R. Liang, E. Zhang, L. Zhang, and Y. Liu, Phys. Rev. B **73**, 155316 (2006).
[15] S. Kettemann, Phys. Rev. Lett. **98**, 176808 (2007).
[16] A. W. Holleitner, V. Sih, R. C. Myers, A. C. Gossard, and D. D. Awschalom, Phys. Rev. Lett. **97**, 036805 (2006).
[17] S. Bandyopadhyay and M. Cahay, *Introduction to Spintronics* (CRC, Boca Raton, FL, 2008).
[18] A. Zunger, Phys. Status Solidi A **190**, 467 (2002).
[19] J. W. Luo, A. N. Chantis, M. van Schilfgaarde, G. Bester, and A. Zunger, Phys. Rev. Lett. **104**, 066405 (2010).
[20] L. W. Wang, J. Kim, and A. Zunger, Phys. Rev. B **59**, 5678 (1999).
[21] L. W. Wang and A. Zunger, Phys. Rev. B **51**, 17398 (1995).
[22] J. W. Luo, G. Bester, and A. Zunger, Phys. Rev. Lett. **102**, 056405 (2009).
[23] As we found in 2D QWs (Ref. 19), the SS of VB1 is a result of both the quantum confinement effect and interband coupling between heavy-hole and light-hole subbands. The cubic SS term of VB1 is complicated and not interesting.
[24] Here the cubic Dresselhaus term coefficient of the conduction band of 3D bulk GaAs is 21.6 rather than 8.3 eV Å^3 fitted to the *GW* result (Ref. 22). This 3D cubic coefficient is close to the value of (110)-oriented 1D wire as shown in Fig. 4(b).
[25] α_{VB1} is 130, 320, and 497 meV Å for wire radius $R = 3$, 4, and 5 nm, respectively.
[26] G. F. Koster, J. O. Dimmock, R. G. Wheeler, and H. Statz, *Properties of the Thirty-Two Point Groups* (MIT Press, Cambridge, MA, 1963).